Supplementary Table S1: Description of the marker locations placed on the body.

Trunk	
LSH	14mm marker over tip of left shoulder (AC joint)
RSH	14mm marker over tip of right shoulder (AC joint)
C7	14mm marker over spinous process of 7th cervical vertebra
T7	14mm marker over spinous process of 7th thoracic vertebra
MAN	14mm marker over manubrium of thoratic cage
Pelvis	
RASI	14mm marker placed over right anterior superior iliac spine (ASIS)
LASI	14mm marker placed over left anterior superior iliac spine (ASIS)
SACR	14mm marker placed over midpoint between left and right posterior superior iliac spines (PSIS)
Right Thigh	
RTHAP	14mm marker located at the proximal anterior aspect of the right thigh
RTHAD	14mm marker located at the distal anterior aspect of the right thigh
RTHLP	14mm marker located at the proximal lateral aspect of the right thigh (upper end of thermoplastic bar)
RTHLD	14mm marker located at the proximal distal aspect of the right thigh (lower end of thermoplastic bar)
RLEPI	14mm marker over lateral epicondyle of right femur
RMEPI*	14mm marker over medial epicondyle of right femur
Left Thigh	
LTHAP	14mm marker located at the proximal anterior aspect of the left thigh
LTHAD	14mm marker located at the distal anterior aspect of the left thigh
LTHLP	14mm marker located at the proximal lateral aspect of the left thigh (upper end of thermoplastic bar)
LTHLD	14mm marker located at the proximal distal aspect of the left thigh (lower end of thermoplastic bar)
LLEPI	14mm marker over lateral epicondyle of left femur
LMEPI*	14mm marker over medial epicondyle of left femur
Right shank	
RTIAP	14mm marker located on the proximal 1/3 of the anterior shaft of the right tibia
RTIAD	14mm marker located on the distal 1/3 of the anterior shaft of the right tibia
RTILAT	14mm marker located on the mid lateral aspect of the right tibia
RLMAL	14mm marker located over the right lateral malleolus
RMMAL*	14mm marker located over the right medial malleolus
Left Shank	
LTIAP	14mm marker located on the proximal 1/3 of the anterior shaft of the left tibia
LTIAD	14mm marker located on the distal 1/3 of the anterior shaft of the left tibia
LTILAT	14mm marker located on the mid lateral aspect of the left tibia
LLMAL	14mm marker located over the left lateral malleolus
LMMAL*	14mm marker located over the left medial malleolus
Right foot	
RHEEL	14mm marker on distal aspect of bisection of right posterior calcaneum
RMID	14mm marker on medial right midfoot
RLATMID	14mm marker on lateral right midfoot
RP1MT	14mm marker on medial aspect of right 1st MTP joint
RP5MT	14mm marker on lateral aspect of right 5th MTP joint
RTOE	14mm marker on distal end of 1st toe of right foot
Left foot	
LHEEL	14mm marker on distal aspect of bisection of left posterior calcaneum
LMID	14mm marker on medial left midfoot
LLATMID	14mm marker on lateral left midfoot
LP1MT	14mm marker on medial aspect of left 1st MTP joint
LP5MT	14mm marker on lateral aspect of left 5th MTP joint
LTOE	14mm marker on distal end of 1st toe of left foot
Right arm	
RARM	14mm marker located at the half way point laterally on the right humerus
RELB	14mm marker over lateral epicondyle of right humerus
RFOREARM	14mm marker located at the half way point laterally on the right forearm
RWR	14mm marker over dorsal aspect of right wrist
Left arm	
LARM	14mm marker located at the half way down laterally on the left humerus
LELB	14mm marker over lateral epicondyle of left humerus
LFOREARM	14mm marker located at the half way point laterally on the left forearm
LWR	14mm marker over dorsal aspect of left wrist

* Markers required for static calibration trial only

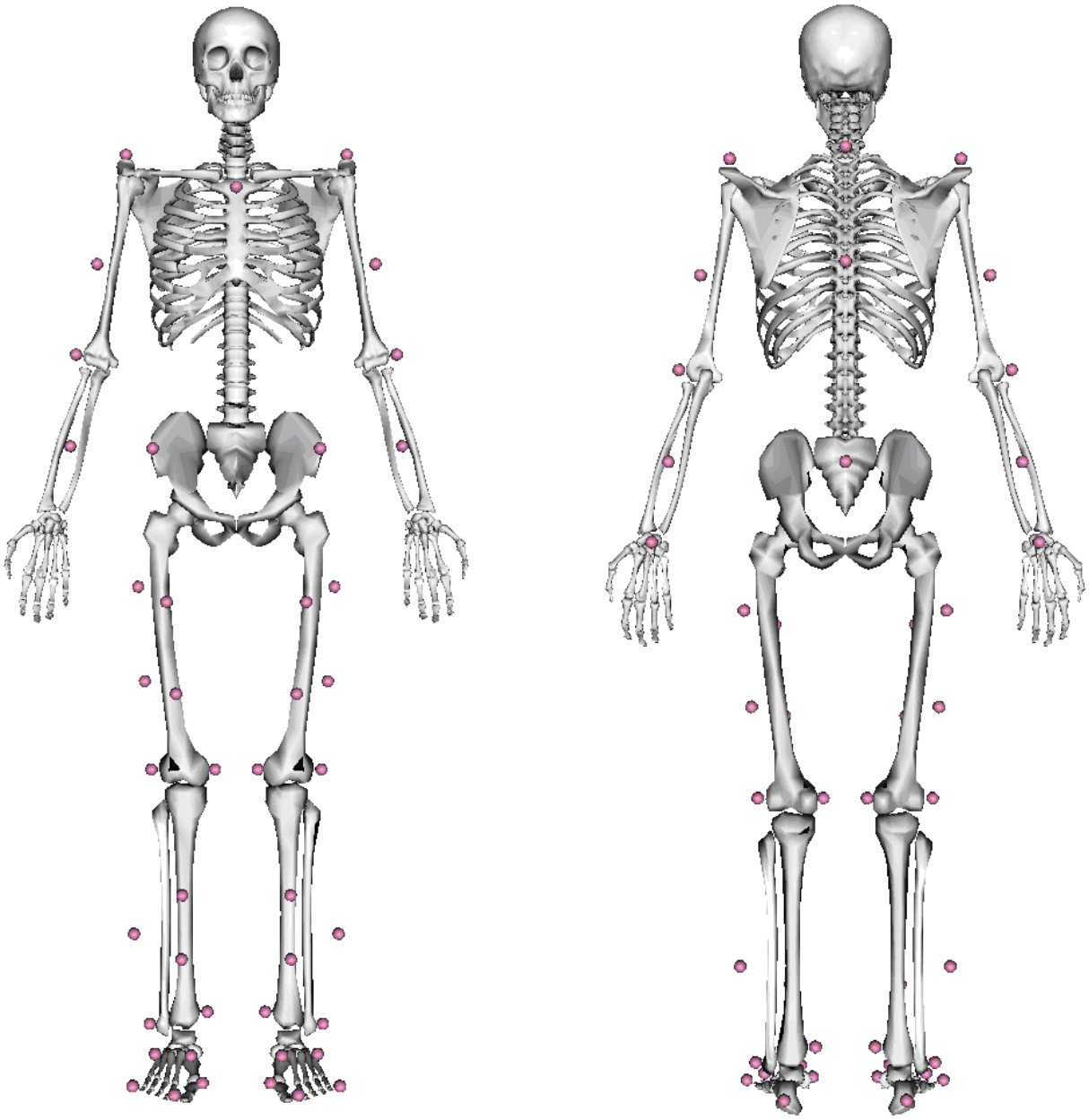

Supplementary Figure S1: Anterior and posterior views of the marker set used in the running gait trials. Forty-six markers were attached to the subject (15 markers on each leg, 4 markers on each arm, and 8 markers on the torso/pelvis).

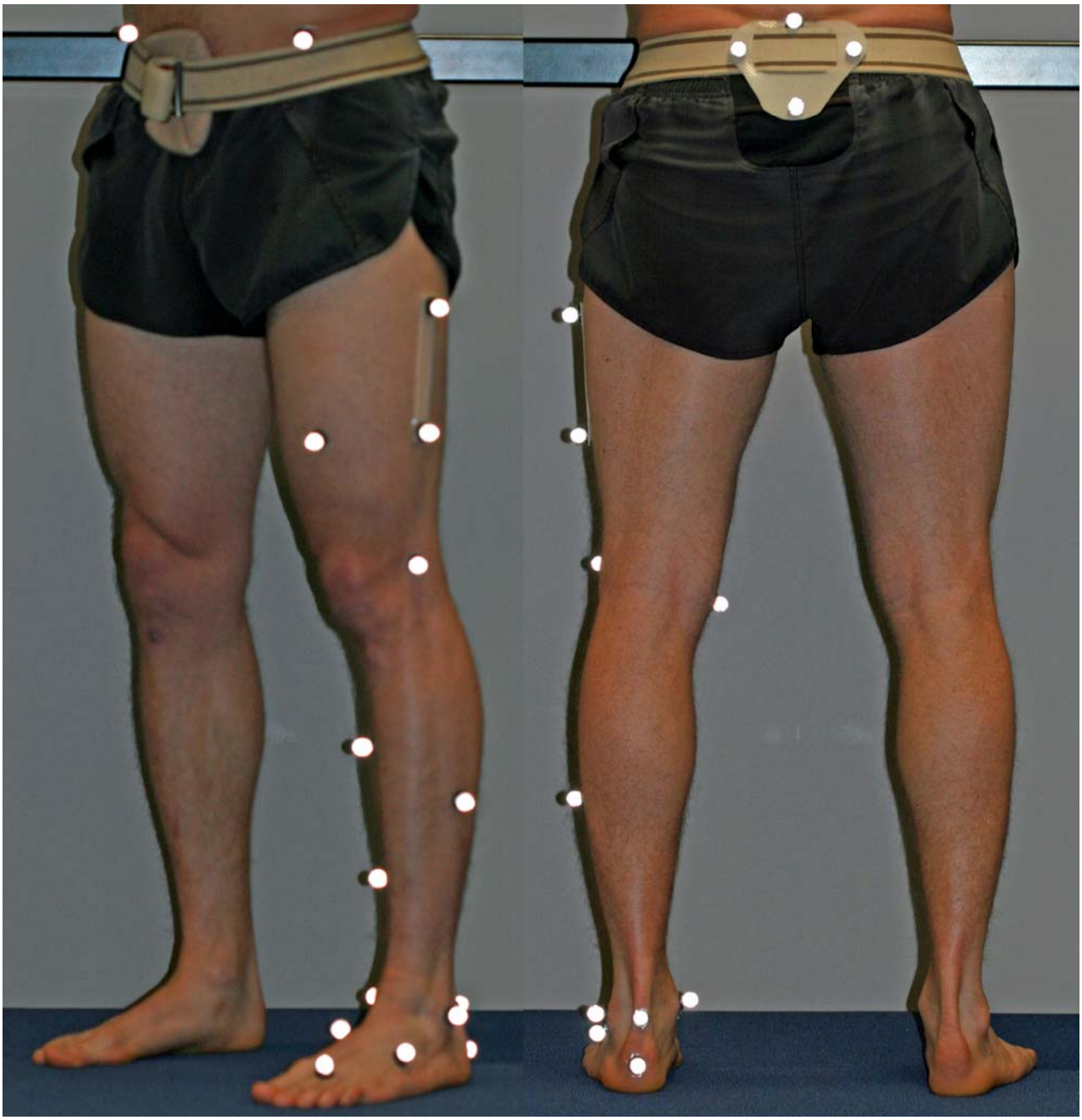

Supplementary Figure S2: Isometric and posterior views of the left lower-limb showing the locations of the skin-mounted markers. Additional markers were placed on the medial malleolus and medial epicondyle of each leg when recording the static standing trial. These additional markers were used to compute the mediolateral femur, tibia and foot lengths. Scale factors were derived from the segment lengths in the axial and mediolateral directions and then used to scale the femur, tibia and foot segments of the model.

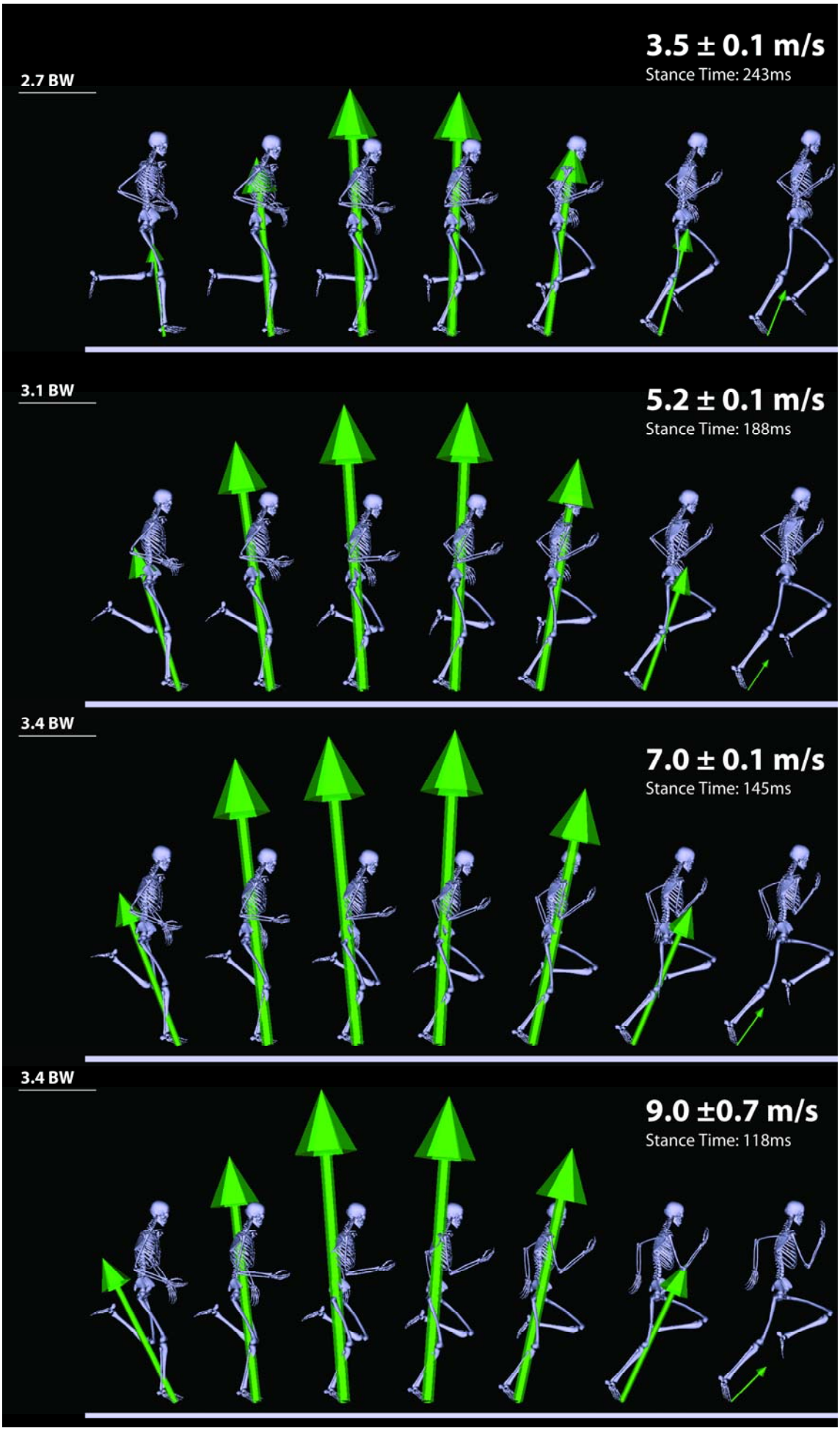
2.7 BW
3.5 ± 0.1 m/s
Stance Time: 243ms
3.1 BW
5.2 ± 0.1 m/s
Stance Time: 188ms
3.4 BW
7.0 ± 0.1 m/s
Stance Time: 145ms
3.4 BW
9.0 ±0.7 m/s
Stance Time: 118ms

Supplementary Figure S3: Sagittal plane view of the joint kinematics and ground reaction forces measured during the stance phase of the stride for one representative subject at the four running speeds tested. Snapshots were taken at equal intervals of the stance phase with the right leg in contact with the ground. The vertical scale represents the peak magnitude of the vertical ground reaction force measured in multiples of body weight (BW).

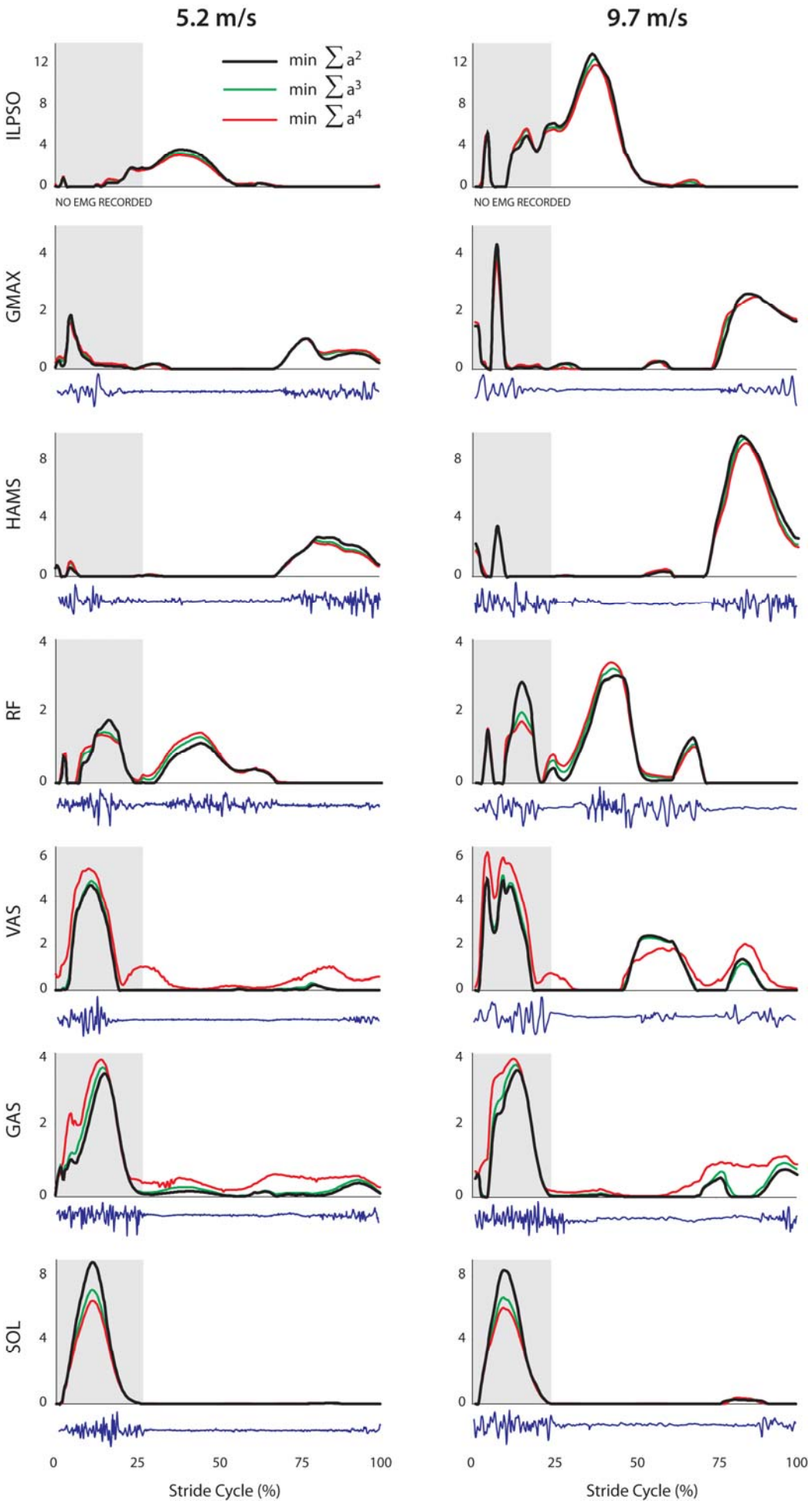
5.2 m/s
9.7 m/s
min $\sum a^2$
min $\sum a^3$
min $\sum a^4$
ILPSO
NO EMG RECORDED
NO EMG RECORDED
GMAX
HAMS
RF
VAS
GAS
SOL
0
25
50
75
100
Stride Cycle (%)
Stride Cycle (%)

Supplementary Figure S4: Sensitivity of muscle force predictions to the cost function exponent for one representative subject running at 5.2 m/s and 9.7 m/s. Force magnitudes were normalized by body weight. Raw EMG signals measured in the experiment are shown below each plot. Muscle symbols appearing in the graphs are: ILPSO (iliacus and psoas combined; no EMG data recorded), GMAX (superior, middle and inferior gluteus maximus), HAMS (biceps femoris long head, semimembranosus and semitendinosus combined, medial hamstring EMG shown), RF (rectus femoris), VAS (vastus medialis, vastus intermedius and vastus lateralis combined; vastus lateralis EMG shown), GAS (medial and lateral compartments of gastrocnemius combined; medial gastrocnemius EMG shown) and SOL (soleus). Because activation dynamics was neglected in the model, there is no time lag between muscle activation and force production; hence at any given time, muscle activations are directly proportional to muscle force.

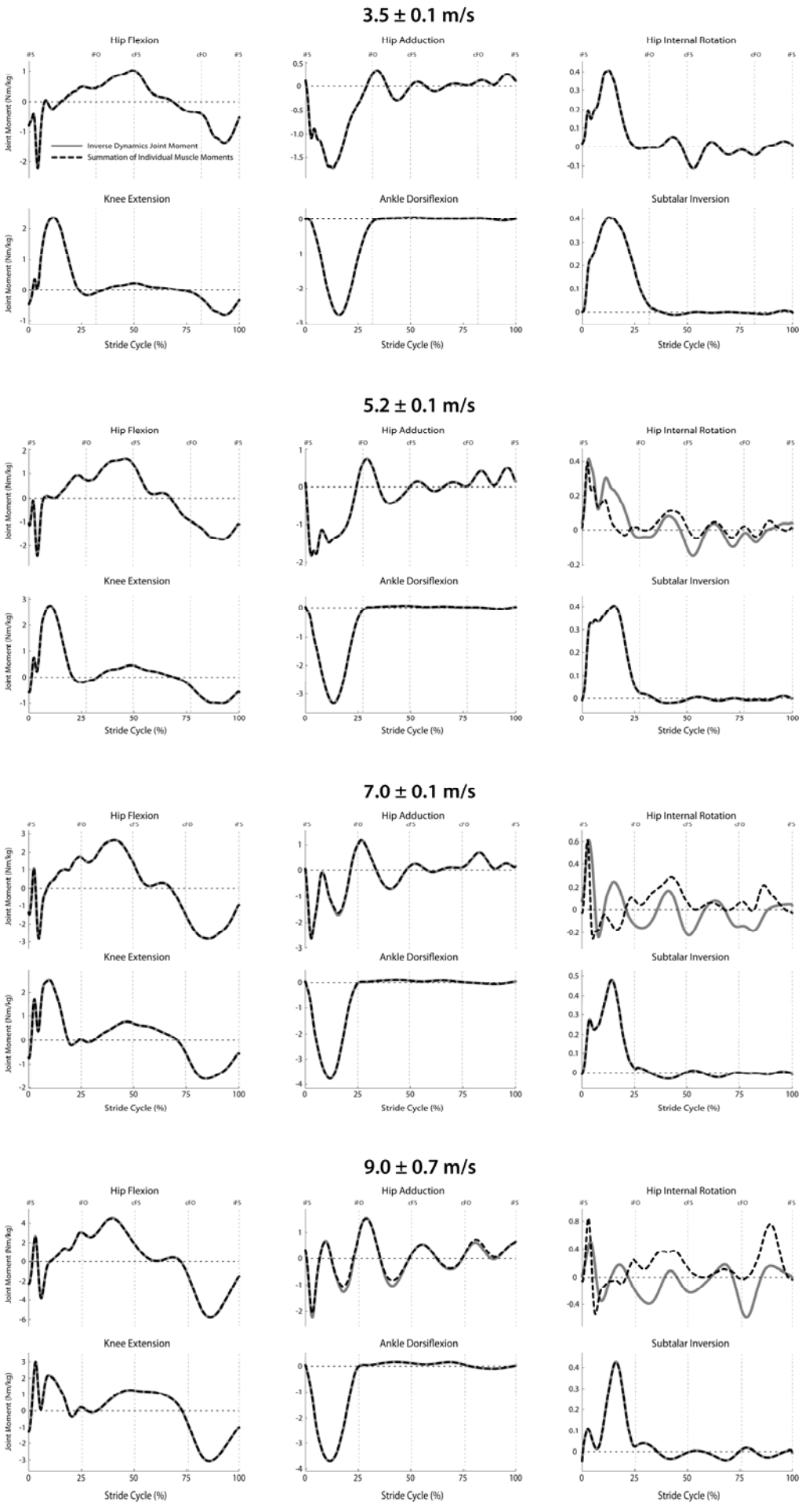
3.5 ± 0.1 m/s
5.2 ± 0.1 m/s
7.0 ± 0.1 m/s
9.0 ± 0.7 m/s
Hip Flexion
Hip Adduction
Hip Internal Rotation
Knee Extension
Ankle Dorsiflexion
Subtalar Inversion
Inverse Dynamics Joint Moment
Summation of Individual Muscle Moments
Joint Moment (Nm/kg)
Stride Cycle (%)
iFS
iFO
cFS
cFO

Supplementary Figure S5: Lower-limb joint moments for each running speed calculated from inverse dynamics (solid line) and by summing the individual moment contributions (product of muscle force from static optimization and moment arm) for every muscle in the model (dashed line). The inverse dynamics solution represents the desired moments that muscles should generate; hence, differences between the two curves indicate where muscles were incapable of satisfying the entirety of the recorded motion. iFS, iFO, cFS and cFO signify ipsilateral foot-strike, ipsilateral foot-off, contralateral foot-strike and contralateral foot-off, respectively.

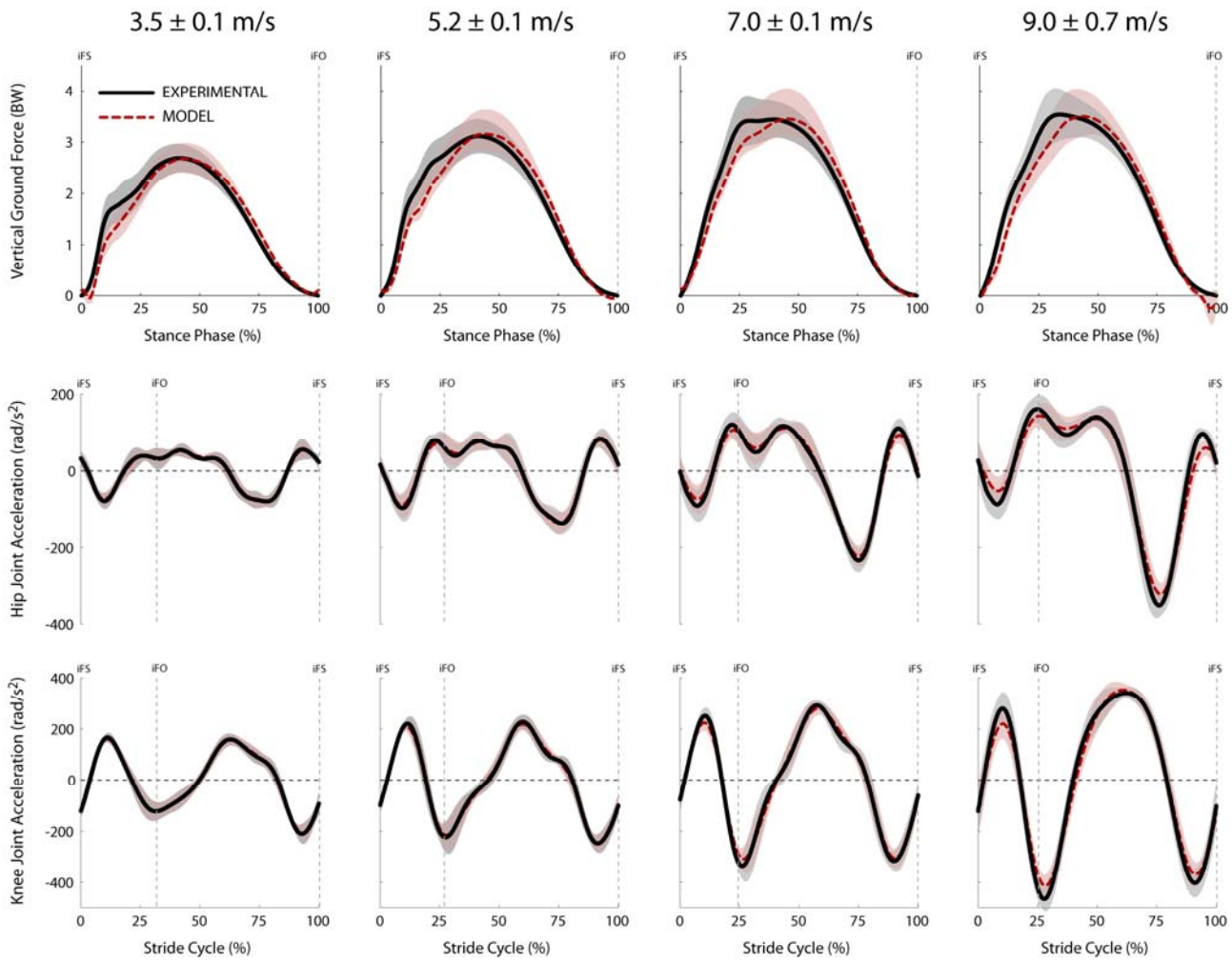

Supplementary Figure S6: Experimental (solid) and model predicted (dashed) trajectories of the vertical ground reaction force, net sagittal hip joint acceleration and net sagittal knee joint acceleration at all running speeds. The vertical ground reaction force is presented during the stance phase, while the hip and knee joint accelerations are presented for the entire stride cycle. Solid and dashed represent mean values across all subjects, and the shaded regions represent one standard deviation from the mean. iFS and iFO signify ipsilateral foot-strike and ipsilateral foot-off, respectively.